

# Three-dimensional Morphogenetic Model of Ice Accretion on a Non-rotating Cylinder

E. B. Lébatto, M. Farzaneh & E. P. Lozowski\*

NSERC / Hydro-Quebec / UQAC Industrial Chair on Atmospheric Icing of Power Network Equipment (CIGELE) and Canada Research Chair on Engineering of Power Network Atmospheric Icing (INGIVRE)  
Université du Québec à Chicoutimi, Chicoutimi, Québec, Canada, G7H 2B1  
Phone: (418) 545-5044; Fax: (418) 545-5032; Web site: <http://cigele.ca>

\*Department of Earth and Atmospheric Sciences, University of Alberta,  
Edmonton, T6G 2E3, Canada

**Keywords:** *freezing rain, ice accretion, ice loads, ice shape, icicle*

**Abstract-** Freezing rain or drizzle may cause severe disruptions of power transmission. It is thus important, in order to alleviate that problem, to find a way to estimate icing intensity over a wide range of conditions and to predict the formation of extreme ice loads. This paper introduces a 3D random walk model for predicting the profile and mass of ice accretion on a non-rotating cylinder. The water film, which flows along the ice or conductor surface, is divided into fluid elements assumed to follow a random path. Three parameters are associated with the random walk model : the probability of freezing and the motion parameter, both dependent on atmospheric conditions, and the shedding parameter, which is a constant.

## I. INTRODUCTION

Freezing rain impingement on power network equipment may cause harmful effects in cold climate regions around the world. Mitigation of these detrimental consequences requires further research including field and laboratory investigations as well as theoretical analysis and computer simulation. Existing computer models of ice accretion on a cylinder, while useful in the past are in need of improvement.

The aim of the present work is to develop a 3D model of ice accretion on a non-rotating cylinder simulating real-life flexibility constraints as shown in Figure 1. This model will simulate the shape and load of accreted ice. The shape of accreted ice will significantly affect the ice load rate of formation.

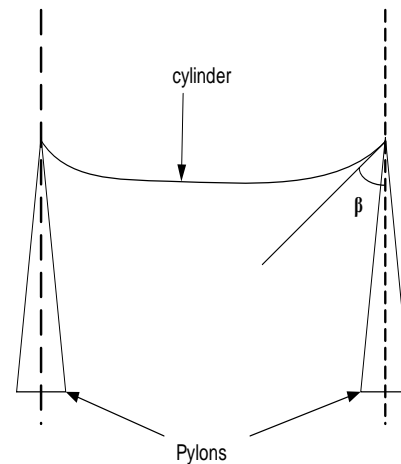


Fig.1 The flexibility of the cylinder represented by angle  $\beta$

Random walk modelling was introduced into the icing domain by Szilder (1, 2). This method allows the simulation of wet icing when unfrozen water flows along the surface of the ice accretion before freezing. Typically, such wet icing is the result of freezing rain. Using this technique, Szilder et al. have also developed a 3D model predicting icicle growth (3, 4).

The present 3D model of ice accretion on a non-rotating cylinder is likewise based on random walk modelling, with variable convective heat flux, impingement angle and angle of inclination of the cylinder. The morphogenetic model (1) adds some “realistic” stochastic variability to ice accretion shapes in keeping with experimental observations. This occurs because each simulation is slightly different when a different sequence of random numbers is used, even though the external conditions may be identical.

## II. MODEL DESCRIPTION

In our model, there are two principal sub-models. One is analytical and the other is numerical. The analytical sub-model sets the relationship between the physical parameters and the model parameters, where freezing probability is a function of atmospheric conditions. Water flow along a cylinder or an ice surface is not a continuous process. Frequently the flowing water is observed to form beads which follow circuitous channels as they move around roughness elements on the cylinder surface. The water mass flux is divided into fluid elements which are fired from the upper boundary of the 3D lattice and move randomly along the existing cylinder or ice surface after impact. After calculating the freezing probability and the shedding parameter, a ballistic model determines the trajectory and impact location of a fluid element depending on the impingement angle  $\phi$  (5, 6).

The fluid elements are fired from a random position on the upper boundary of the lattice. Prior to their impact, the particles follow a straight-line trajectory with angle of impact,  $\phi$ . The tangent of this angle is set equal to the ratio of the horizontal wind speed and the terminal velocity of the falling drops (5,6).

$$\phi = \tan^{-1}\left(\frac{V_w}{V_T}\right) \quad (1)$$

where  $V_w$  ( $\text{m.s}^{-1}$ ) is the wind speed;  $V_T$  is the terminal velocity of the droplets ( $\text{m.s}^{-1}$ ).

The terminal velocity of a droplet, based on the data of Gunn and Kinzer (7), is expressed as follows

$$V_T = 9.65 - 10.3e^{-0.6D} \quad (2)$$

where  $D$  is the diameter of the raindrop (mm). In reality the impact angle varies with raindrop size, even with constant wind. However, in the present work we have fixed the raindrop size while varying the impingement angle. To determine the moving probability of motion of a fluid element in any direction we assumed that: at any step of its random walk, the freezing probability remains constant; fluid elements are fired from random position on the upper boundary of the 3D lattice; the probability that a fluid particle will move one cell upwards is zero; in the absence of wind, the angle between the stagnation line and the raindrop's trajectory is zero; when the impingement angle is zero, the five motion probabilities are all equal; the ratio of the difference between the probability that a fluid element will move one cell downwind and the probability that a fluid element will move one cell upwind and the probability that a fluid particle will move one cell downward is the tangent of the raindrop impingement angle  $\phi$ ; the inclination angle of the cylinder due its flexibility is  $\beta$ .

Any fluid element has a volume of  $1\text{mm}^3$  after freezing. The simulation domain is defined by a 3D rectangular lattice. The icing substrate is defined by filling up appropriate lattice cells. In this 3D model, at each time step during the random walk, a fluid element has six possible alternatives. Either it moves one cell to right, left, down, downstream, upstream (diagonal motion is not allowed), or it freezes. A probability is associated with each event as will be defined in upcoming

sections. In addition, the particle is not allowed to walk away from the substrate or the ice structure. While flowing along the surface, a particle's behaviour has two possible outcomes, either it merges with the existing accretion when it freezes, or it drips from the accretion. Particle freezing occurs on drawing a random number whose value is within the freezing probability interval. However, a fluid element will not necessarily freeze in its present lattice cell. A "cradle" location is sought for this element in the neighborhood of its current cell. The size of this neighborhood is determined by the freezing range parameter,  $n$ . At present, the freezing range parameter is taken to be 2, in agreement with the numerical experiments of Szilder (4), which gave a correspondence with observed porosity. The neighborhood is a square of side  $2n+1$  cells. Within this area, the particle moves to the empty cell that has the maximum number of occupied neighbors. If the cells which meet this condition are several, the final location is chosen randomly. This process emulates the effect of the surface tension force that tends to minimize the local surface area.

Due to the lack of a complete analysis in 3D, we have used the 2D analytical model of Szilder (1) to calculate the freezing probability. Next we have deduced the motion probability in each direction taking into account the 3D lattice. Szilder showed that the freezing probability which is proportional to the net external heat transfer can be expressed as follows:

$$P_f = \frac{\pi Q \Delta x P_c}{2 m_0 L_f} \quad (3)$$

where  $Q$  is the mean convective heat flux ( $\text{W.m}^{-2}$ );  $\Delta x$  is the step length measured along the cylinder surface;  $R$  is the cylinder radius;  $L_f$  is the latent heat of fusion ( $\text{J.kg}^{-1}$ );  $m_0$ : the total mass flux of impinging drops onto the cylinder when the rainfall is vertical,  $wR$  ( $\text{kg.m}^{-1}.\text{s}^{-1}$ ), with  $w$  being the rainfall rate ( $\text{kg.m}^{-2}.\text{s}^{-1}$ ). As we can see, the freezing probability has been expressed as function of the convective heat flux, precipitation rate, the lattice cell size, and cylinder radius. This expression remains constant during the ice accretion for simplicity. The second parameter of this model is the shedding parameter. It emulates the behaviour of a pendant drop. If a fluid element moves along the iced cylinder surface without freezing, it will eventually reach the icicle's tip. If it remains at the tip without freezing for the number of times steps defined by the shedding parameter, it drips and leaves the ice structure. Physically, this parameter is related to the supply rate. However, no attempt will be made to derive a relation in this paper. Instead, the shedding parameter is estimated at 500 using previous work (1, 5, and 6).

Figure 2 shows a cross-section of the cylinder showing its inclination angle. When the cylinder is inclined the probability of motion towards the right ( $P_{ZR}$ ) and downward ( $P_{YD}$ ) are obtained through a projection of their value on  $Z$  and  $Y$  axis respectively when the cylinder is not inclined.

The probability of motion towards the left is set equal to the sum of  $P_{ZL}$  when  $\beta$  is equal  $90^\circ$  with the difference between the probabilities  $P_{YD}$  and  $P_{ZR}$  when  $\beta$  is equal  $90^\circ$ . When the cylinder is not inclined and the rainfall is vertical, the probabilities of motion in each of the five possible directions are identical may be expressed as follows:

$$P_{Mo} = \frac{1 - P_c}{5} \quad (4)$$

Taking into account the impingement angle of the raindrops, we can write:

$$\begin{cases} \frac{P_{Xds} - P_{Xus}}{P_{Mo} \cos \phi} = \tan \phi \\ P_{Xds} - P_{Xus} = 1 - P_c - P_{Mo} \cos \phi - 2 P_{Mo} \end{cases} \quad (5)$$

In resolving the equation system (5) we obtain:

$$\begin{cases} P_{Xds} = P_{Mo} \frac{(3 + \sin \phi - \cos \phi)}{2} \\ P_{Xus} = P_{Mo} \frac{(3 - \sin \phi - \cos \phi)}{2} \end{cases} \quad (6)$$

Considering the slope of the cylinder represented by  $\beta$  (figure2), the probability that a liquid particle moves one cell downward becomes:

$$P_D = P_{Mo} \cos \phi \sin \beta \quad (7)$$

Then we define the probabilities remaining.

$$\begin{aligned} P_{ZR} &= P_{Mo} \sin \beta \\ P_{ZL} &= P_{Mo} (2 - \sin \beta + \cos \phi - \cos \phi \sin \beta) \end{aligned} \quad (8)$$

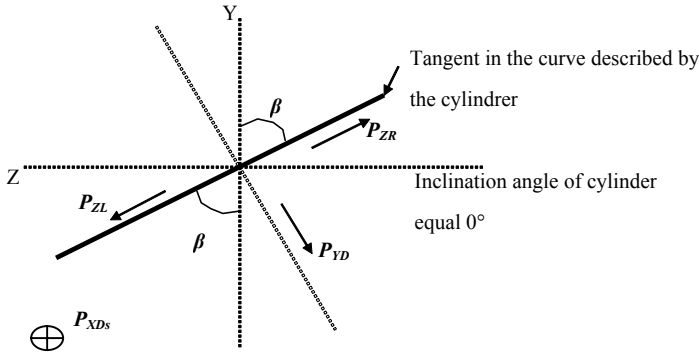


Fig.2 Cylinder viewed from the side showing its inclination

### III. MODEL SIMULATION RESULTS AND DISCUSSION

Simulations were run on a 3D lattice consisting of 200 by 150 by 200 cubic grid cells, each with 1mm sides. In this model, the influence of external heat flux, impingement angle and inclination angle of the cylinder have been investigated. In general, the external heat flux consists of convective, evaporative and radiative sources but we have condensed all these terms into a single term for simplification. Freezing rain is often accompanied by wind. In general, the wind speed and its direction vary with time. These parameters influence the impingement angle of the droplets, but for simplicity a fixed value is assigned to the impact angle which is assumed to remain constant during the simulation.

#### A. Influence of the convective heat flux

In this section, the following values are assumed:  $\beta=90^\circ$ , the rainfall rate  $1\text{mmh}^{-1}$ , the simulation time 5h and the cylinder radius 17.5 mm. The rainfall is vertical.

The influence of the convective heat flux on ice accretion shape is shown in figure 3. In this figure, different shapes of ice accretion are presented. For figures 3.a and 3.b where the convective heat flux is  $2\text{W.m}^{-2}$  and  $5\text{W.m}^{-2}$  respectively, ice does not cover the entire cylinder surface. Also we see that ice tends to accumulate below the cylinder. Availability of heat and water below the cylinder leads to a substantial accretion there. For higher values of convective heat flux, as we can see in figures 3.e and 3.f, there is more ice accreted on the cylinder's upper surface and hence a decrease of the length of the icicles. When the convective heat flux is high, there is substantial heat lost to the cold air and the freezing probability is therefore higher, causing droplets to freeze just after their impact. In summary, the lower values of convective heat flux lead to some smaller icicles, and an increase of the heat flux produce an increase of icicle length. However, for the highest values of convective heat flux the icicles become smaller because all the raindrops freeze on the cylinder itself. This observation is in agreement with Maeno and Takahashi's experimental data (8, showing that decreasing air temperature leads to longer icicles). Finally, after reaching a maximum length, a further increase of the heat flux or a decrease of the air temperature, leads to shortening of the icicles.

The influence of the convective heat flux on the distribution of the mass is shown in figure 4. Accretion mass grows with increasing external convective heat flux. The total impinging rainfall mass also increases slowly with increasing heat flux, since the cross-section of the accretion increases with the external heat flux, figure 3. When the convective heat flux reaches  $140\text{Wm}^{-2}$ , the total ice accretion mass and the total impinging rainfall mass are almost equal. This may be explained by the fact that when the convective heat flux is very high, all the impinging water is incorporated into the ice structure and there is virtually no dripping.

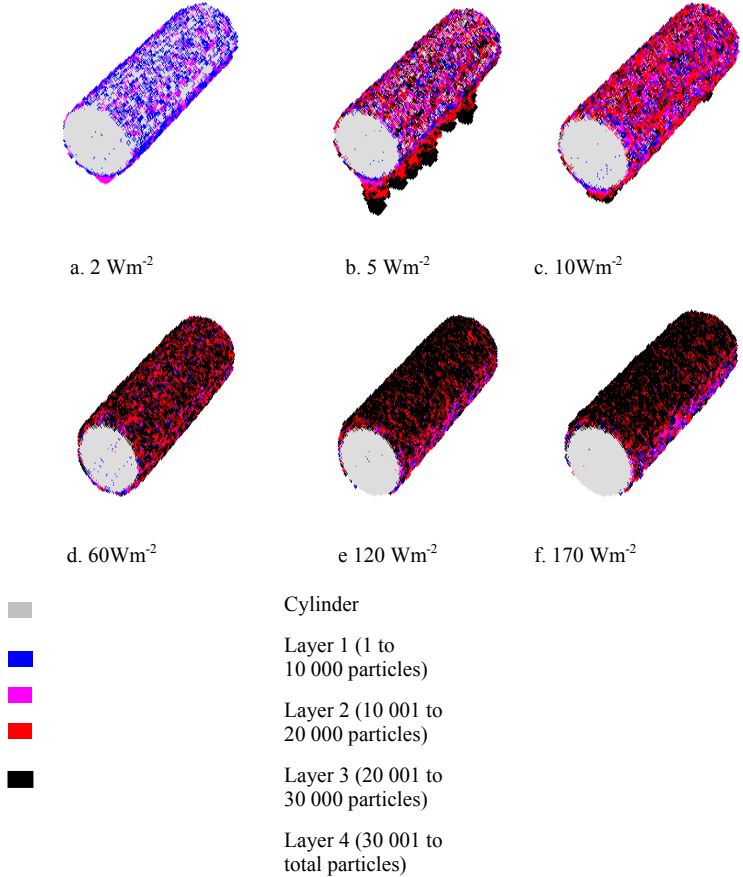


Fig.3. The influence of convective-heat flux on the shape of the ice accretion. The following parameter values have been assumed: rainfall rate, 1 mmh<sup>-1</sup>; simulation time 5 hours; the shedding parameter, 500; the impingement angle  $\Phi$  is set equal to 0°; the inclination angle  $\beta$  is set equal to 90°.

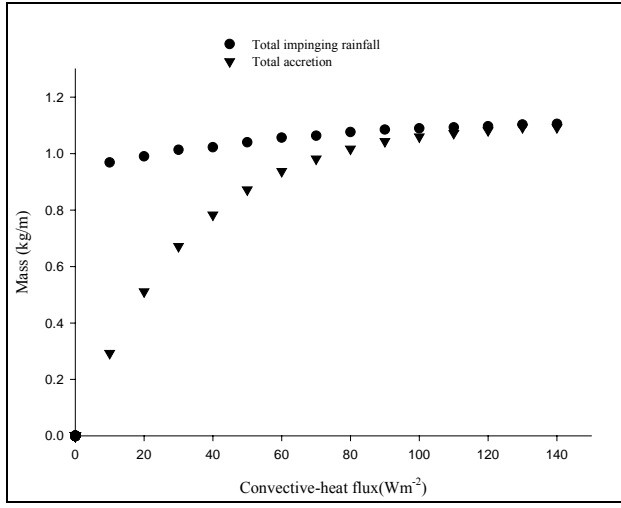


Fig.4. The influence of convective-heat flux on the distribution of ice mass during the accretion process. Rainfall rate 5 mmh<sup>-1</sup>; simulation time 5 hours; the shedding parameter, 500; the impingement angle  $\Phi$  is set equal to 0°; the inclination angle  $\beta$  is set equal to 90°.

*B. Influence of the impingement angle*

It has been established that the heat transfer coefficient and the impact angle will both depend on wind speed. For convenience, however, we have kept the external heat flux constant while changing the impingement angle, in order to identify their individual effects. The range of the angle of impact was chosen according to Chen (5,6). The mono disperse raindrop impingement angle varies from approximately 20° to 70°. For this range, the simulation results for accretion shape are shown in figure 5. The following values have been assumed: the convective heat flux 5 Wm<sup>-2</sup>, simulations time 5 hours,  $\beta = 90^\circ$ . The right side is the upstream side. It is clear that ice accretion preferentially occurs on the upwind side of the existing ice structure as the raindrop impingement angle increases. It so happens because this side is more exposed to the freezing rain. The icicle formation process here is the same as what was described in the previous section, with the difference that, in this section, we have a downwind inclination of the icicles.

The distribution of ice accretion mass is presented in figure 6. The total accretion mass increases with increasing impingement angle until it reaches its maximum at around 60°. This increase comprises two stages, from 0° to 20°, and from 20° to 60°. In the first stage, the mass increase is slow because it is caused by a slow increase of the cylinder surface which is exposed to the wind. For the higher values of the impact angle the variation of the cylinder surface which is exposed is significant, hence there is a faster increase of the total accretion mass in the second part. Beyond 60°, a slight decrease of the total accretion mass is observed. An increase of total accretion mass should rather be expected, considering the increase of the lateral cross-section of the ice structure directly exposed to raindrop spraying. This is explained by the fact that this lateral cross-section is not a curtain of ice; hence, for very high values of impingement angle, a fraction of the droplets passes between the icicles below the cylinder, leading to a decrease of the total accretion mass.

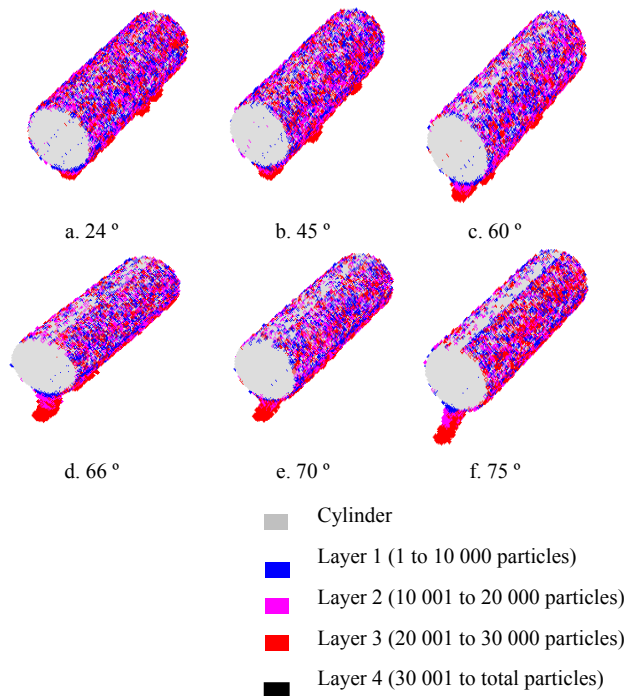


Fig.5 The influence of raindrop impingement angle on the shape of the ice accretion. The following parameter values have been assumed: rainfall rate,  $1\text{mmh}^{-1}$ ; simulation time 5 hours; convective heat flux  $5\text{W.m}^{-2}$ ; the shedding parameter 500; the inclination angle  $\beta$  is set equal to  $90^\circ$ .

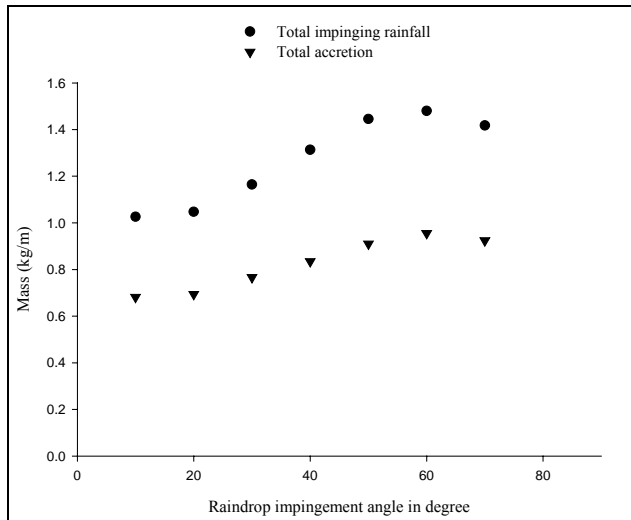


Fig.6 The influence of the raindrop impingement angle on the total ice mass during the accretion process. Convective-heat flux  $30\text{Wm}^{-2}$ ; rainfall rate  $5\text{mmh}^{-1}$ , simulation time 5 hours.

C. Influence of the inclination angle of the cylinder

Figure 7 presents the influence of the inclination angle of the cylinder on the icing process in the wet regime. A decrease of this angle, starting from  $90^\circ$ , leads to a slight increase of the mass intercepted until  $50^\circ$ , followed by a significant increase thereafter. At the same time there is a slight decrease followed by a significant increase of the ice accreted mass. For an inclination angle less than  $50^\circ$ , the liquid particles quickly reach the bottom of the ice structure under the influence of gravity. This explains the slight decrease of the accreted mass.

When the inclination angle is greater than  $50^\circ$ , the opposite phenomenon is observed, namely an increase of the ice mass. This is so because, after their impact, the raindrops move on in the direction of the slope of the cylinder, thus spending more time on the ice structure with a higher probability of freezing on the structure.

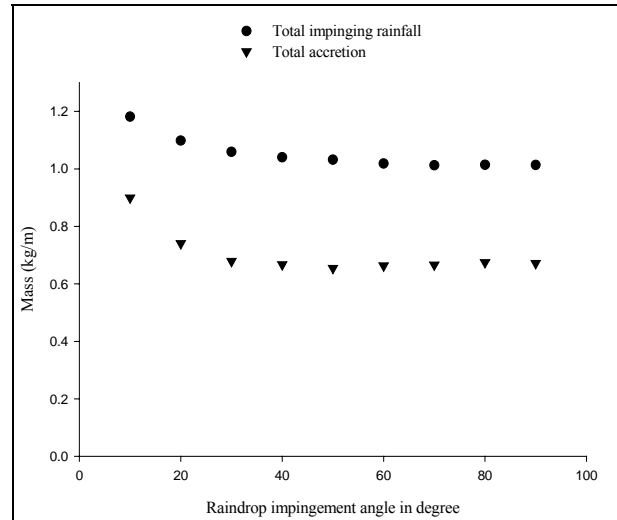


Fig. 7.a\*

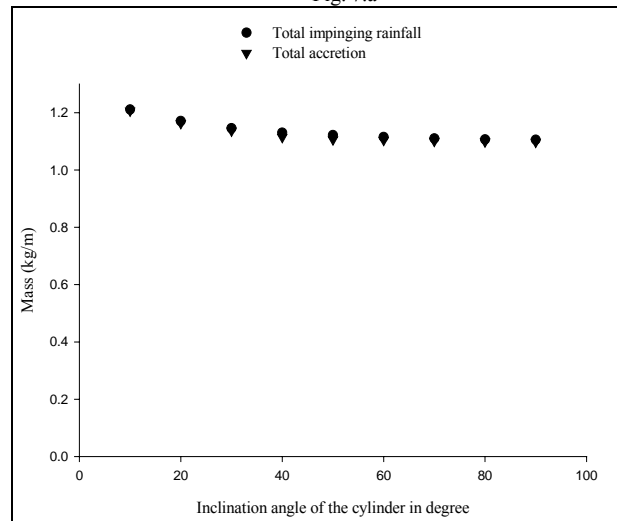


Fig. 7.b\*\*

Fig. 7 The influence of the cylinder inclination angle  $\beta$  on the distribution of ice mass during the accretion process. The following parameter values have been used: rainfall rate  $5\text{mmh}^{-1}$ ; simulation time 5 hours; the shedding parameter, 500; the impingement angle  $\Phi$  is set equal to  $0^\circ$ .

(\*) Wet case (convective-heat flux  $30\text{Wm}^{-2}$ )  
 (\*\*) Dry case (convective-heat flux  $140\text{Wm}^{-2}$ ).

At an angle of  $90^\circ$ , 66 % of the raindrops intercepted by the cylinder or by the ice mass are incorporated into the ice accretion. For smaller angles, the intercepted mass of water grows slowly while the accreted ice mass decreases slowly until  $50^\circ$ . At this angle, there is a decrease of 2.5% in accreted ice mass compared to  $90^\circ$ . From  $50^\circ$  to  $10^\circ$ , there is a 40 % increase of the accreted ice mass, relative to  $90^\circ$ .

Figure 7.b describes the influence of the cylinder inclination angle on the icing process in the dry regime, when

there is no dripping or icicle formation. The curves describing the accreted ice mass and the intercepted water mass are almost identical. The external heat flux is sufficient to incorporate almost the totality of the intercepted raindrops into the ice accretion.

#### IV. CONCLUSIONS

The morphogenetic model is in qualitatively good agreement with observations in terms of its simulation of ice accretion due to freezing rain on a cylinder. The shape and the mass of the ice accretion can be predicted by the model, while changing the droplet impingement angle, the convective heat flux and the inclination angle of the cylinder. In future, we hope that it will lead to even more realistic predictions when we include the impact of the wind on the heat transfer at the cylinder surface. The results to be reported in a future paper will be verified with laboratory experiments.

#### V. ACKNOWLEDGEMENTS

This research was carried out within the framework of the NSERC/Hydro-Quebec Industrial Chair on Atmospheric Icing of Power Network Equipment (CIGELE) and the Canada Research Chair on Atmospheric Icing Engineering of Power Network (INGIVRE) at Université du Québec à Chicoutimi (UQAC) in collaboration with the University of Alberta. The authors would like to thank all the sponsors of the project for their financial support. In particular, we thank the Canadian Foundation for Climate and Atmospheric Sciences for a generous research grant.

#### VI. REFERENCES

- [1] K. SZILDER, 1993. The density and structure of ice accretion predicted by a random-walk model, *Quarterly Journal of the Royal meteorological Society*, Vol 119, N° 513, pp.907-924.
- [2] K. SZILDER, 1994. Simulation of ice accretion on a cylinder due to freezing rain. *Journal of Glaciology*, Vol 40, N°136, pp.586-594.
- [3] K. SZILDER, E. P. LOZOWSKI, 1994. Stochastic modeling of icicle formation. *Journal of Offshore Mechanics and Arctic Engineering*, Vol 116, pp.180-184.
- [4] K. SZILDER, E. P. LOZOWSKI, 1995. Simulation of icicle growth using a three-dimensional random walk model. *Atmospheric Research*, Vol 36, pp.243-249.
- [5] Y. CHEN, M. FARZANEH, E. P. LOZOWSKI, 2001. Modeling of ice accretion on transmission line conductor. *Proceedings 9<sup>th</sup> International Workshop on Atmospheric Icing of structures, Chester, June 2000*, 8pp.
- [6] Y. CHEN, 2001. A 2-D random walk model for predicting ice accretion on a cylindrical conductor. *MSc Thesis, Université du Québec à Chicoutimi*, ISBN 0-612-65271-8, 82pp.
- [7] GUNN, R, KINSER, G.D., 1949. The terminal velocity of fall for water droplets in stagnant air. *Journal of Meteorology*. Vol 6, pp.243-248.

- [8] N.MAENO, T.TAKAHASHI, 1984. Studies on icicles. I. General aspects of the structure and growth of icicles, *Low Temp Sci Ser A*, Vol 43, N° 6, pp. 125-138.